The Surprising Dynamics of the McLafferty Rearrangement

Jacob Stamm, Sung Kwon, Shawn Sandhu, Moaid Shaik, Rituparna Das, Jesse Sandhu, Bradley Curenton, Clayton Wicka, Benjamin G. Levine, Liangliang Sun, and Marcos Dantus*

Read Online

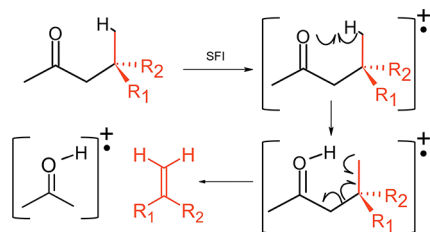ACCESS | Metrics & More | Article Recommendations | Supporting Information

ABSTRACT: We report femtosecond time-resolved measurements of the McLafferty rearrangement following the strong-field tunnel ionization of 2-pentanone, 4-methyl-2-pentanone, and 4,4-dimethyl-2-pentanone. The pump–probe-dependent yields of the McLafferty product ion are fit to a biexponential function with fast (~100 fs) and slow (~10 ps) time constants, the latter of which is faster for the latter two compounds. Following nearly instantaneous ionization, the fast time scale is associated with rotation of the molecule to a six-membered cyclic intermediate that facilitates transfer of the γ-hydrogen, while the ~50–100 times longer time scale is associated with a π-bond rearrangement and bond cleavage between the α- and β-carbons to produce the enol cation. These experimental measurements are supported by *ab initio* molecular dynamics trajectories, which further confirm the time scale of this important stepwise reaction in mass spectrometry.
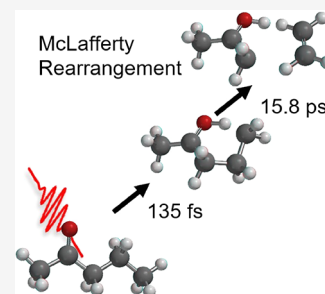
Presently, *ab initio* prediction of the fragmentation patterns that aid in the identification of compounds in mass spectrometry remains a challenge.[1–3] The energy gained by a molecule during electron ionization is sufficient to trigger multiple reactions with tens of different products. However, their associated time scales remain largely unknown. Revealing the ultrafast time scales of the multiple competing reaction pathways following electron ionization would be beneficial to better understand the processes that lead to the observed fragmentation pattern. This information could help refine theories aimed at predicting the branching ratios among the competing reactions occurring during the fragmentation of radical cations far from equilibrium and aid in molecular design to control the yield of specific fragment ions.

One of the better known fragmentation mechanisms in mass spectrometry is the McLafferty rearrangement.[4] As shown in Scheme 1, the McLafferty rearrangement occurring in radical cations is characterized by a γ-hydrogen transfer to a double-bonded atom through a six-membered transition state followed by β-carbon bond cleavage to produce a neutral olefin. First noticed in aliphatic acids, ketones, and aldehydes,[4–7] the rearrangement was found to be analogous to the Norrish type II reaction in neutrals.[6] While some studies have considered it to be a concerted mechanism,[8–10] there is abundant evidence for a stepwise mechanism.[11–13] The product formed by aliphatic ketones was identified as an enol cation because it is more stable than a ketone cation, whereas the opposite is true for neutral molecules.[14–16] Interestingly, the enol to ketone isomerization occurs in a nonergodic process leading to the loss of the newly formed methyl group.[17,18] The appearance of nonergodic products in mass spectrometry[19] is difficult to predict via statistical methods such as quasi-equilibrium theory[20] and Rice–Ramsperger–Kassel–Marcus theory.[21,22] Nonergodic processes have the potential to break strong chemical bonds while leaving weak bonds intact, with important applications in post-translational modification mapping in proteomics.[23] Time-resolved studies of the Norrish type II reaction on 2-pentanone, 2-hexanone, and 5-methyl-2-hexanone have been carried out, with results suggesting a stepwise mechanism with a fast (70–90 fs) H transfer followed by a slow (400–700 fs) cleavage.[24] Here we focus on the time-resolved dynamics of the McLafferty rearrangement, with

Scheme 1. Generalized McLafferty Rearrangement Mechanism of a Methyl Ketone Initiated by Strong-Field Ionization (SFI)[a]

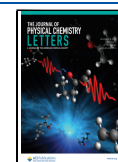[a]In this study, R_1 and R_2 are H and H in 2-pentanone, H and CH_3 in 4-methyl-2-pentanone, and CH_3 and CH_3 in 4,4-dimethyl-2-pentanone.

sufficient time resolution to distinguish between nonsynchronous concerted and stepwise mechanisms.[25]

Here we measure the time scales of the McLafferty rearrangement reaction (Scheme 1) in 2-pentanone, 4-methyl-2-pentanone, and 4,4-dimethyl-2-pentanone. For the time-resolved measurements, an 800 nm, 35 fs Ti:sapphire laser compressed by multiphoton intrapulse interference phase scan (MIIPS)[26] is split into two pulses with peak intensities of 1×10^{14} W/cm^2 and 4×10^{13} W/cm^2, respectively. The pump pulse singly ionizes (Figures S1 and S2) the molecules via tunnel ionization (Table S1), depositing tens of electronvolts of energy into the molecule and initiating the McLafferty rearrangement. The time-delayed probe pulse disrupts product formation.[27] Note that once the reaction is complete, the probe pulse can no longer appreciably affect the yield of the products. By scanning the time delay between the pump and probe pulses, one can measure the fragmentation dynamics following ionization. During our measurements, unimolecular reaction conditions are ensured by the lack of molecular clusters and because the mean time between molecular collisions is 10 orders of magnitude longer than the experiment time (50 ps) and 4 orders of magnitude longer than the time to detection. Additionally, to ensure that our results are relevant to electron ionization mass spectrometry (EI-MS), the intensity of the pump pulse was attenuated until the resulting mass spectrum resembled the mass spectrum obtained via EI-MS,[28] and thus, the energy deposited into the molecule was similar to that deposited during 70 eV EI-MS (see Figure S3). The mass spectrum contains the ion yields of all of the thermodynamically possible reactions. Both reaction pathway selection and the time constant depend on the internal energy gained during ionization, which for electron ionization as well as for ultrafast ionization used here is quite broad (10–20 eV).[29] Finally, the time between ionization and detection, which in our case is ≤10 μs, must also influence the observed fragmentation pattern. The McLafferty rearrangement product yields for pump-only strong-field ionization (SFI) and EI-MS are shown in Table 1. From the similarities between the McLafferty product ion yields obtained by the two methods, we confirm that SFI provides similar internal energy to the molecules as EI-MS.
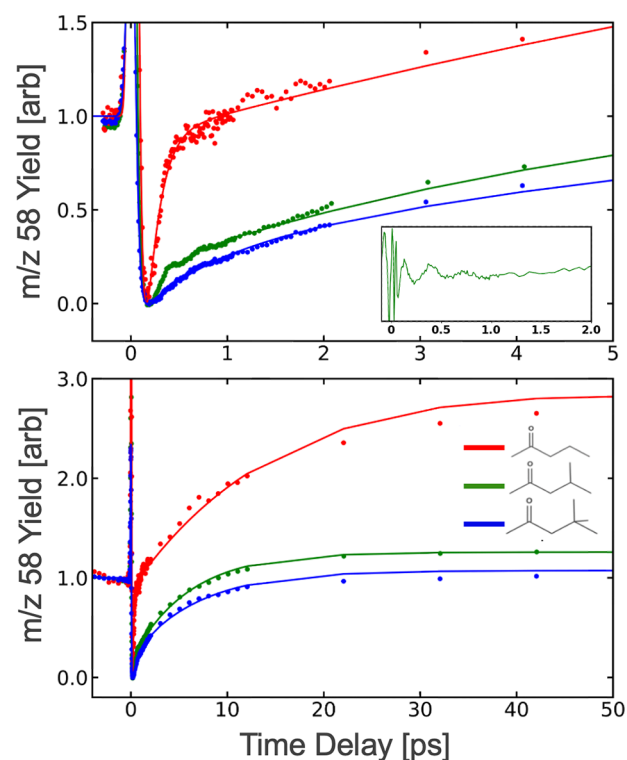
Table 1. Measured Yields of the McLafferty Rearrangement Product Ion (m/z 58) from Pump-Only ($\sim 1 \times 10^{14}$ W/cm^2) Strong-Field Ionization and 70 eV EI-MS (NIST)[a]

compound	SFI	NIST[28]
2-pentanone	0.02	0.05
4-methyl-2-pentanone	0.10	0.12
4,4-dimethyl-2-pentanone	0.14	0.11

[a]Yields have been normalized to the sum of all ions above m/z 14. SFI mass spectra of the three compounds can be found in Figure S3.

Time-resolved measurements for three different methyl ketones track the yield of the m/z 58 ion, which corresponds to the McLafferty product, as a function of pump−probe delay. The time-dependent data are listed in Figure 1.

The time-dependent yield was fitted to the following function, derived in other works.[27] Since the data show both fast and slow components, two exponential rise terms were included in the fitting function, along with a decay term following time zero and an offset term:

Figure 1. Pump−probe dependent ion yields of the McLafferty rearrangement product (m/z 58) for 2-pentanone (red), 4-methyl-2-pentanone (green), and 4,4-dimethyl-2-pentanone (blue). Dots indicate experimental points, and lines indicate fits using eq 1. An additional term was added to the curve fit to account for the oscillatory behavior. Yields have been normalized so the minimum of the depletion is 0 and yield at negative times is 1. The top figure shows the time-dependent curves during the first 5 ps, while the bottom shows the first 50 ps. The inset in the top figure shows the isolated oscillatory behavior of the product yield for 4-methyl-2-pentanone.

$$P(t) = a\mathrm{e}^{-t^2/s^2} + bP_1(t, \tau_{\mathrm{decay}}) + cP_2(t, \tau_{\mathrm{rise}_1})$$
$$+ dP_3(t, \tau_{\mathrm{rise}_2}) + eP_4(t, \tau_{\mathrm{offset}}) + fS(t, \tau_{\mathrm{damp}}) \quad (1)$$

where

$$P_i(t, \tau_i) = \mathrm{e}^{-t/\tau_i}\left[1 + \mathrm{erf}\left(\frac{t}{s} - \frac{s}{2\tau_i}\right)\right] \quad (2)$$

and

$$S(t, \tau_{\mathrm{damp}}) = \mathrm{e}^{-t/\tau_{\mathrm{damp}}}\left[\cos\left(\frac{2\pi t}{f_0 t + T}\right)\right] \quad (3)$$

Here the constants τ_{rise_1} and τ_{rise_2} indicate the time scales of the dynamics of the McLafferty rearrangement, a−e are amplitude coefficients, τ_{decay} describes the decay following the time-zero spike, and τ_{offset} accounts for asymmetry in yield between negative and long positive time delays. The frequency-swept sinusoidal term $S(t, \tau_{\mathrm{damp}})$ was included only when fitting 4-methyl-2-pentanone to account for coherent oscillations. In this term, τ_{damp} is the damping time constant for the oscillations, T is the period, and f_0 is the constant that describes the frequency sweep. The two time scales that describe the McLafferty rearrangement (τ_{rise_1}, τ_{rise_2}) of each

compound are summarized in Table 2. It should be noted that the data in Figure 1 are normalized for visual aid. The extracted

Table 2. Measured Time Scales of the McLafferty Rearrangement Product Ion for 2-Pentanone, 4-Methyl-2-pentanone, and 4,4-Dimethyl-2-pentanone[a]

| compound	τ_1 (fs)	τ_2 (ps)
2-pentanone	135 ± 30	15.8 ± 1.5
4-methyl-2-pentanone	186 ± 5	5.90 ± 0.73
4,4-dimethyl-2-pentanone	916 ± 180	7.35 ± 0.85

[a]Results were obtained with the pump pulse intensity adjusted to match the EI-MS results. Coefficients correspond to the τ's in eq 1 and are shown with ±95% error bars. Coefficients of the full fit can be found in Table S2.

time scales from eq 1 are independent of this normalization. Additionally, 2-pentanone had an additional P_i term to account for dynamics at long (≥50 ps) positive time delays. While these results are for low (1×10^{14} W/cm²) pump intensity, it should be noted that when the pump pulse that initiates the dynamics is of a higher intensity (5×10^{14} W/cm²), more energy can be deposited into the molecule, affecting the yields and time scales (see Figures S4 and S5 and Table S3).

The complex interplay between fragmentation channels responsible for the observed mass spectrum can be resolved by direct measurement of their time scales. One can gain perspective on the values compiled in Table 2 by comparing the time scales of the McLafferty rearrangement to simpler reactions such as α- or β-carbon bond cleavage. In Figure 2, we show the time-dependent yields of two of these competing fragmentation channels in 4,4-dimethyl-2-pentanone following strong (5×10^{14} W/cm²) pump ionization, a condition where we can associate the dynamics to α and β cleavage individually. The fast time constants of the α and β cleavage channels under these conditions are ~150 and ~500 fs, respectively. These time scales correlate to the yields of their products (m/z 43 = 20% and m/z 57 = 3%) under these conditions. The variation in time scales and stabilities of these competing pathways affects the yield of the McLafferty rearrangement. Considering the fast time scale of the α and β channel products, one can understand their higher yields as they compete with the slower McLafferty rearrangement, which takes several picoseconds to complete.

We propose the following explanation for the observed time scale and yield trends of the McLafferty rearrangement for the three compounds studied here. Regarding the τ_1 time scale, it reports on the bond rotation necessary to attain the critical cyclic geometry and the hydrogen transfer. Upon ionization, the cyclic geometry is a more stable configuration than the linear geometry.[13] Attaining this geometry requires torsional motion because prior to ionization most molecules are far from the cyclic structure (see Figure S6). This time scale is relatively fast due to the downhill potential energy surface along this reaction coordinate.[13] We attribute the τ_1 time scale to the time for the molecules to rotate to the cyclic geometry and undergo proton transfer. This time scale is consistent with prior studies of gas-phase proton transfer time scales.[24,30]

The τ_2 time scale, which is about 50–100 times slower than τ_1, reports on the β-carbon bond cleavage. We find a significant decrease in the τ_2 time scale between 2-pentanone and the branched ketones (see Table 2). To gain further insight into the measured time scales, *ab initio* molecular dynamics
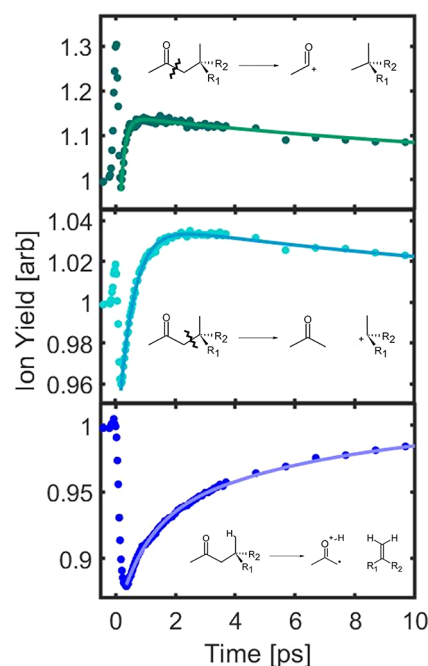
Figure 2. Pump−probe-dependent ion yields of the α bond cleavage product (m/z 43) in green, the β bond cleavage product (m/z 57) in light blue, and the McLafferty rearrangement product (m/z 58) in dark blue. Dots indicate experimental points, and lines indicate biexponential fits. Ionization was initiated following irradiation with a strong (5×10^{14} W/cm²) pump. All curves are shown for 4,4-dimethyl-2-pentanone, with R_1 = CH$_3$ and R_2 = CH$_3$. This was required because the other two compounds under study have overlapping peaks for the α and β cleavage channels or no presence of the β cleavage. Yields have been normalized so that the yield at negative times is 1. The α cleavage channel has a fast time scale of ~150 fs, while the β cleavage channel has a fast time scale of ~500 fs.

(AIMD) trajectories of the photodissociation of singly ionized 2-pentanone and 4-methyl-2-pentanone were conducted at the roωB97/6-31++G** level.[31−33] From these calculations, we observed that the McLafferty rearrangement always occurs via a stepwise mechanism with a fast formation of the six-membered cyclic transition state and proton transfer step followed by a slower bond cleavage and enol cation formation step (see the Supporting Information and Supporting Videos 1, 2, and 3). It is the long τ_2 time scale that we find to be surprising. If this step required exclusively electronic motion, then it would be completed a few orders of magnitude faster. Instead, we find experimentally and through examination of AIMD trajectories that this step requires significant exploration of multiple internal degrees of freedom to reach the molecular geometry that enables the π-electron rearrangement. In other words, the molecular wave function explores the multidimensional potential energy surface until it finds the transition state responsible for π-electron rearrangement and dissociation into an enol and olefin. This vibrational control of an ostensibly pure electronic motion parallels the Marcus picture of electron transfer.[34] This process depends on the total amount of energy available and the rate of the intramolecular vibrational energy redistribution (IVR). The τ_2 time scale is faster when the product is a substituted ethylene because the IVR rate depends on the density of states and therefore increases with the addition of methyl groups. These two facts explain why the τ_2 time scale is ~2 times faster for the methyl-substituted 2-pentanones.
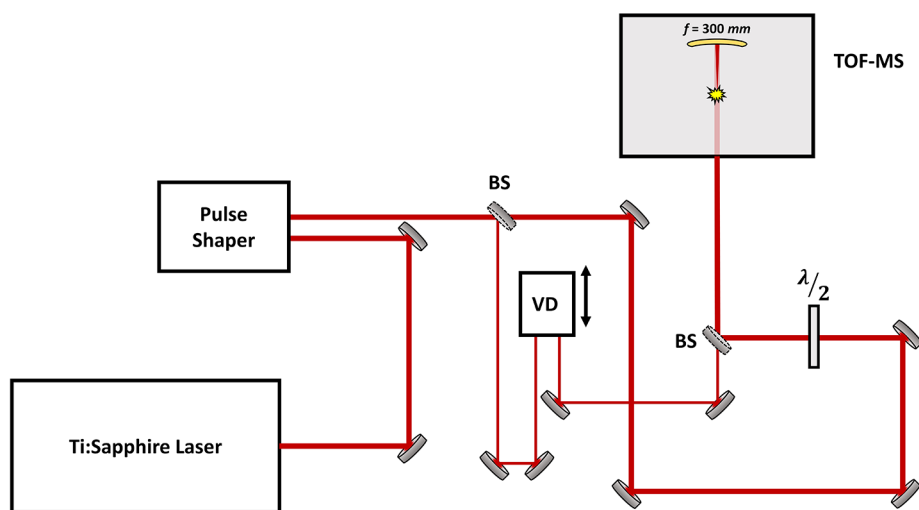
Figure 3. Experimental setup of a pump−probe scheme for disruptive probing measurements. Abbreviations: BS, beam splitter; VD, variable delay stage; TOF-MS, time-of-flight mass spectrometer.

In conclusion, we present femtosecond time-resolved studies of the McLafferty rearrangement in 2-pentanone, branched 4-methyl-2-pentanone, and 4,4-dimethyl-2-pentanone. These measurements were made possible by ultrafast disruptive probing, a method capable of following tens of reaction pathways synchronously.[27] We find that the main ionic product of this reaction reflects two time scales. The first time scale is associated with the internal rotation necessary to achieve the six-membered cyclic structure that facilitates the proton transfer. The second and ∼50−100 times slower time scale is associated with bond rearrangement and β-carbon bond cleavage. Measurement of simpler reaction pathways involving a single bond cleavage, such as α bond cleavage, revealed much faster dynamics. Ultrafast time-resolved studies of fundamental reactions of radical cations far from equilibrium, such as this one, inform efforts to predict fragment ion yields following electron ionization mass spectrometry. Identifying critical competing pathways and transition states by this type of study can also help control product yields via molecular design.

EXPERIMENTAL SECTION

The compounds 2-pentanone, 4-methyl-2-pentanone, and 4,4-dimethyl-2-pentanone were purchased from Millipore Sigma at ≥98% and used without further purification. We employed a Wiley−McLaren time-of-flight (TOF) mass spectrometer[35] and an amplified femtosecond laser pulse as the excitation source (Figure 3). The samples to be studied were freeze−pump−thawed and introduced to the TOF chamber as an effusive beam through a needle valve. The pressure in the chamber was kept at 2×10^{-6} Torr during data collection, and when the valve was closed, the pressure quickly dropped to 5×10^{-8} Torr. To ionize the molecules, a 35 fs, 800 nm pulse from a Ti:sapphire regeneratively amplified laser was used. These pulses were generated at a 1 kHz repetition rate and had a pulse energy of 1 mJ, directly out of the amplifier. Pulses were then sent to a pulse shaper running the multiphoton intrapulse interference phase scan (MIIPS) software, which corrects all orders of the spectral phase distortions present in the pulses.[26] The deviation from transform-limited pulses was kept below 0.2% for all measurements. After pulse compression, the pulses were split into a strong pump (1×10^{14} W/cm^2) and a weak probe (4×10^{13} W/cm^2) using a beam splitter. The intensities at the focus were calibrated using the ratio of doubly to singly ionized argon.[36] For yield measurements, the probe was blocked, so that only the strong pump interacted with the molecules inside the chamber. The probe pulse was sent to a variable delay stage so that the time delay between the pump and probe pulses could be controlled with femtosecond resolution. These pulses were then recombined using a beamsplitter and sent into the TOF chamber, where a 300 mm gold-coated back-focusing mirror was used to focus the beam. Molecules in the focus were then ionized and sent to a microchannel plate detector by a +2168 V repeller plate and a +1080 V extractor plate separated by 10 mm. Note that with this setup only cations were detected. Ion signals originating at the microchannel plate detectors were then digitized in an oscilloscope and stored in a computer for later analysis and processing.

The main method used to measure the dynamics and time scales of the McLafferty rearrangement is called disruptive probing.[27] Here the probe pulse is scanned in time using the delay stage, and the yield of each ion in the mass spectrum is tracked as a function of the time delay between the pump and probe pulses. While the pump pulse is strong enough to ionize and fragment the target molecules, the probe pulse can only disrupt the formation of an ion as it is in the process of being formed. The probe pulse cannot form ions on its own and does not appreciably affect the ions once they have been formed. Since ions generally cannot be further fragmented by the probe pulse but are susceptible to yield changes during their formation, the yields seen in the pump−probe delay curves measure the molecular dynamics that leads to a particular ion. Ions whose formation is disrupted cause a corresponding increase in yield of several other product ions. Thus, the probe pulse couples ion channels during the transient states of the molecule during fragmentation but not appreciably afterward.

ASSOCIATED CONTENT

Ⓢ Supporting Information

The Supporting Information is available free of charge at https://pubs.acs.org/doi/10.1021/acs.jpclett.3c02102.

Details regarding the instrumentation and experiment setup, extra time-resolved data, mass spectra of the

compounds, and further explanation on data interpretation (PDF)

Transparent Peer Review report available (PDF)

Supporting Video 1: 2-pentanone (AVI)

Supporting Video 2: 4-methyl-2-pentanone (fast) (AVI)

Supporting Video 3: 4-methyl-2-pentanone (slow) (AVI)

■ AUTHOR INFORMATION

Corresponding Author

Marcos Dantus − *Department of Chemistry, Michigan State University, East Lansing, Michigan 48824, United States; Department of Physics and Astronomy, Michigan State University, East Lansing, Michigan 48824, United States;* ⊙ orcid.org/0000-0003-4151-5441; Email: dantus@chemistry.msu.edu

Authors

Jacob Stamm − *Department of Chemistry, Michigan State University, East Lansing, Michigan 48824, United States*

Sung Kwon − *Department of Chemistry, Michigan State University, East Lansing, Michigan 48824, United States*

Shawn Sandhu − *Department of Chemistry, Michigan State University, East Lansing, Michigan 48824, United States;* ⊙ orcid.org/0000-0001-6252-4270

Moaid Shaik − *Department of Chemistry, Michigan State University, East Lansing, Michigan 48824, United States*

Rituparna Das − *Department of Chemistry, Michigan State University, East Lansing, Michigan 48824, United States*

Jesse Sandhu − *Department of Chemistry, Michigan State University, East Lansing, Michigan 48824, United States*

Bradley Curenton − *Department of Chemistry, Michigan State University, East Lansing, Michigan 48824, United States*

Clayton Wicka − *Department of Chemistry, Michigan State University, East Lansing, Michigan 48824, United States*

Benjamin G. Levine − *Department of Chemistry and Institute of Advanced Computational Science, Stony Brook University, Stony Brook, New York 11794, United States;* ⊙ orcid.org/0000-0002-0356-0738

Liangliang Sun − *Department of Chemistry, Michigan State University, East Lansing, Michigan 48824, United States;* ⊙ orcid.org/0000-0001-8939-5042

Complete contact information is available at:
https://pubs.acs.org/10.1021/acs.jpclett.3c02102

Notes

The authors declare no competing financial interest.

■ ACKNOWLEDGMENTS

■ REFERENCES

(1) Allen, F.; Pon, A.; Greiner, R.; Wishart, D. Computational Prediction of Electron Ionization Mass Spectra to Assist in GC/MS Compound Identification. *Anal. Chem.* **2016**, *88*, 7689−7697.

(2) Ji, H.; Deng, H.; Lu, H.; Zhang, Z. Predicting a Molecular Fingerprint from an Electron Ionization Mass Spectrum with Deep Neural Networks. *Anal. Chem.* **2020**, *92*, 8649−8653.

(3) Collins, S. L.; Koo, I.; Peters, J. M.; Smith, P. B.; Patterson, A. D. Current Challenges and Recent Developments in Mass Spectrometry-Based Metabolomics. *Annu. Rev. Anal. Chem.* **2021**, *14*, 467−487.

(4) McLafferty, F. W. Mass Spectrometric Analysis. Molecular Rearrangements. *Anal. Chem.* **1959**, *31*, 82−87.

(5) Happ, G. P.; Stewart, D. W. Rearrangement Peaks in the Mass Spectra of Certain Aliphatic Acids. *J. Am. Chem. Soc.* **1952**, *74*, 4404−4408.

(6) Nicholson, A. J. C. The Photochemical Decomposition of the Aliphatic Methyl Ketones. *Trans. Faraday Soc.* **1954**, *50*, 1067−1073.

(7) Gilpin, J.; McLafferty, F. Mass spectrometric analysis aliphatic aldehydes. *Anal. Chem.* **1957**, *29*, 990−994.

(8) Fairweather, R.; McLafferty, F. Formation of $[M—C_2H_4]^{+\bullet}$ in O-d_1-Butyric Acid. *Org. Mass Spectrom* **1969**, *2*, 755−756.

(9) Allison, C. E.; Stringer, M. B.; Bowie, J. H.; Derrick, P. J. Combined Deuterium and Oxygen-18 Isotope Effects in Support of a Concerted, Synchronous Elimination of Acetaldehyde from a Bis(Benzyl Ethyl Ether) Radical Cation. *J. Am. Chem. Soc.* **1988**, *110*, 6291−6297.

(10) Trigueros, P. P.; Casanovas, J.; Alemán, C.; Vega, M. C. A MNDO and AM1 Quantum Chemical Study of the Reaction Mechanism of the McLafferty Type Rearrangement in the Butanal Radical Cation. *J. Mol. Struct.* **1992**, *277*, 117−127.

(11) Smith, J. S.; McLafferty, D. F. Evidence for a Stepwise Mechanism for the γ-Hydrogen Rearrangement. *Org. Mass Spectrom.* **1971**, *5*, 483−485.

(12) Kingston, D. G.; Bursey, J. T.; Bursey, M. M. Intramolecular Hydrogen Transfer in Mass Spectra. II. McLafferty Rearrangement and Related Reactions. *Chem. Rev.* **1974**, *74*, 215−242.

(13) Yasumoto, R.; Matsuda, Y.; Fujii, A. Infrared Spectroscopic Observation of the McLafferty Rearrangement in Ionized 2-Pentanone. *Phys. Chem. Chem. Phys.* **2020**, *22*, 19230−19237.

(14) McLafferty, F.; McAdoo, D.; Smith, J. S.; Kornfeld, R. Metastable Ions Characteristics. XVIII. Enolic $C_3H_6O^+$ Ion Formed from Aliphatic Ketones. *J. Am. Chem. Soc.* **1971**, *93*, 3720−3730.

(15) Holmes, J.; Lossing, F. Heats of Formation of Ionic and Neutral Enols of Acetaldehyde and Acetone. *J. Am. Chem. Soc.* **1982**, *104*, 2648−2649.

(16) Tureček, F.; Hanuš, V. Loss of Methyl from $[H_2C=C(OH)—CH_3]^{+\bullet}$ Ions Prepared by Electron Impact Ionization of Unstable 2-Hydroxypropene. *Org. Mass Spectrom.* **1984**, *19*, 631−638.

(17) McLafferty, F. W.; McAdoo, D. J.; Smith, J. S. Metastable Ion Characteristics. XVI. Ketonization of Gaseous Enol Ions. *J. Am. Chem. Soc.* **1970**, *92*, 6343−6345.

(18) Depke, G.; Lifshitz, C.; Schwarz, H.; Tzidony, E. Non-Ergodic Behavior of Excited Radical Cations in the Gas Phase. *Angew. Chem., Int. Ed. Engl.* **1981**, *20*, 792−793.

(19) McLuckey, S.; Sallans, L.; Cody, R.; Burnier, R.; Verma, S.; Freiser, B.; Cooks, R. Energy-Resolved Tandem and Fourier-Transform Mass Spectrometry. *Int. J. Mass Spectrom. Ion Phys.* **1982**, *44*, 215−229.

(20) Rosenstock, H. M.; Wallenstein, M.; Wahrhaftig, A.; Eyring, H. Absolute Rate Theory for Isolated Systems and the Mass Spectra of Polyatomic Molecules. *Proc. Natl. Acad. Sci. U. S. A.* **1952**, *38*, 667−678.

(21) Rice, O. K.; Ramsperger, H. C. Theories of unimolecular gas reactions at low pressures. *J. Am. Chem. Soc.* **1927**, *49*, 1617−1629.

(22) Marcus, R. A.; Rice, O. The Kinetics of the Recombination of Methyl Radicals and Iodine Atoms. *J. Phys. Chem.* **1951**, *55*, 894−908.

(23) Kalcic, C. L.; Reid, G. E.; Lozovoy, V. V.; Dantus, M. Mechanism Elucidation for Nonstochastic Femtosecond Laser-Induced Ionization/Dissociation: from Amino Acids to Peptides. *J. Chem. Phys. A* **2012**, *116*, 2764−2774.

(24) De Feyter, S.; Diau, E. W.-G.; Zewail, A. H. Femtosecond Dynamics of Norrish Type-II Reactions: Nonconcerted Hydrogen-Transfer and Diradical Intermediacy. *Angew. Chem.* **2000**, *112*, 266−269.

(25) Marvet, U.; Brown, E. J.; Dantus, M. Femtosecond concerted elimination of halogen molecules from halogenated alkanes. *Phys. Chem. Chem. Phys.* **2000**, *2*, 885−891.

(26) Xu, B.; Gunn, J. M.; Cruz, J. M. D.; Lozovoy, V. V.; Dantus, M. Quantitative Investigation of the Multiphoton Intrapulse Interference Phase Scan Method for Simultaneous Phase Measurement and Compensation of Femtosecond Laser Pulses. *J. Opt. Soc. Am. B* **2006**, *23*, 750−759.

(27) Jochim, B.; DeJesus, L.; Dantus, M. Ultrafast Disruptive Probing: Simultaneously Keeping Track of Tens of Reaction Pathways. *Rev. Sci. Instrum.* **2022**, *93*, 033003.

(28) Wallace, W. E. NIST Mass Spectrometry Data Center. In *NIST Chemistry WebBook, NIST Standard Reference Database Number 69*; Linstrom, P. J.; Mallard, W. G., Eds.; National Institute of Standards and Technology, Chapter Mass Spectra.

(29) Grimme, S. Towards First Principles Calculation of Electron Impact Mass Spectra of Molecules. *Angew. Chem., Int. Ed.* **2013**, *52*, 6306−6312.

(30) Ampadu Boateng, D.; Word, M. D.; Gutsev, L. G.; Jena, P.; Tibbetts, K. M. Conserved Vibrational Coherence in the Ultrafast Rearrangement of 2-Nitrotoluene Radical Cation. *J. Phys. Chem. A* **2019**, *123*, 1140−1152.

(31) Chai, J.; Head-Gordon, M. Systematic optimization of long-range corrected hybrid density functionals. *J. Chem. Phys.* **2008**, *128*, 8.

(32) Ufimtsev, I. S.; Martinez, T. J. Quantum Chemistry on Graphical Processing Units. 3. Analytical Energy Gradients, Geometry Optimization, and First Principles Molecular Dynamics. *J. Chem. Theory. Comput.* **2009**, *5*, 2619−2628.

(33) Seritan, S.; Bannwarth, C.; Fales, B. S.; Hohenstein, E. G.; Isborn, C. M.; Kokkila-Schumacher, S. I. L.; Li, X.; Liu, F.; Luehr, N.; Snyder, J. W.; Song, C.; Titov, A. V.; Ufimtsev, I. S.; Wang, L.-P.; Martinez, T. J. TeraChem: A graphical processing unit-accelerated electronic structure package for large-scale ab initio molecular dynamics. *WIREs Comput. Mol. Sci.* **2021**, *11*, 1494.

(34) Marcus, R. A.; Sutin, N. Electron Transfers in Chemistry and Biology. *Biochim. Biophys. Acta, Rev. Bioenerg.* **1985**, *811*, 265−322.

(35) Wiley, W.; McLaren, I. H. Time-of-Flight Mass Spectrometer with Improved Resolution. *Rev. Sci. Instrum.* **1955**, *26*, 1150−1157.

(36) Guo, C.; Li, M.; Nibarger, J. P.; Gibson, G. N. Single and Double Ionization of Diatomic Molecules in Strong Laser Fields. *Phys. Rev. A* **1998**, *58*, R4271.